Ionisation of Rydberg hydrogen atom near a metal surface by short pulse laser*

Wang Lei(汪 磊), Yang Hai-Feng(杨海峰),
Liu Xiao-Jun(柳晓军), and Liu Hong-Ping(刘红平)†

State Key Laboratory of Magnetic Resonance and Atomic and Molecular Physics,Wuhan Institute of Physics and Mathematics, Chinese Academy of Sciences, Wuhan 430071*, China*

(Received 27 May 2010; revised manuscript received 6 July 2010)

In the ionisation of Rydberg hydrogen atoms near a metal surface, the electron will escape from the nucleus and arrive at the detector in a time sequence. This probability flux train relies on the initial electron wave packet irradiated by the laser pulse. For simplicity, the laser pulse is usually simplified to a delta function in energy domain, resulting in a sharp initial arrival time with an exponentially decaying tail at the detector. Actually and semiclassically, the initial outgoing wave should be modeled as an ensemble of trajectories propagating away from the atomic core in all directions with a range of launch times and a range of energies. In this case, each pulse in the pulse train is averaged out rather than a sharp profile. We examine how energy and time averaging of the electron wave packet affects the resolution of escaping electron pulses and study the energy dependence of the arrival time for each pulse in the ionisation train. An optimization condition for the laser pulse shape to generate narrow ionisation electron pulse in the train is obtained. The ionisation rates with various excitation energy are calculated also, which show the excitation to higher N Rydberg states will narrow the electron pulse as well.

Keywords: Rydberg hydrogen, ionisation, trajectory
PACC: 3300, 3370J, 3380E

1. Introduction

Rydberg wave packets are a very useful tool for understanding the crossover between classical and quantum dynamics. They reflect the time evolution of the localized coherent superposition of a system, thus providing a bridge between quantum mechanics and classical concept of trajectories of particles.[1] In the past decades, much attention has been focused on the generation and detection of wave packets in Rydberg atom systems.[2−14] The wave packet dynamics of such systems is qualitatively described by the powerful classical mechanics and semiclassical mechanics, either in the time domain[4,15,16] or in the spatial domain.[17]

Recently, Mitchell *et al.*[4,15] performed a classical calculation to investigate the ionisation of a hydrogen atom in parallel electric and magnetic fields as an example of electron wave packet escape dynamics in an open system in the time domain. The ionisation process can be well described by the following semiclassical picture. When the atom is excited by a short pulse laser, the valence electron is promoted from a low-energy bound state into an outgoing wave which can be modeled semiclassically as an ensemble of trajectories propagating away from the atomic core in all directions with a range of launch times and a range of energies. The wave packet evolves in the Coulomb field of the proton plus the applied electric and magnetic fields. Over the course of time, some of the wave packets slip over the classical barrier, are then drawn downhill by external field, and strike the detector. They observed distributions of electrons ionising via a train of pulses: a consequence of the classical chaos induced by the external magnetic field.[12]

Motivated by the work of Mitchell *et al.*, Wang *et al.*[16] studied the ionisation rate of the Rydberg hydrogen atoms near a metal surface. This is another example of electron wave packet escape dynamics in an open system in the time domain. They find that hydrogen atoms can also ionise through emission of a train of electron pulses but the chaos is induced by the metal surface instead of the external magnetic field. In their semiclassical simulations, a simplified model is adopted to clarify the main dynamic processes: all the trajectories have a fixed energy and are continuously emitted from the source for all times. Eventually, however, for the short pulse laser excitation, the

*Project supported by the National Natural Science Foundation of China (Grant No. 10774162).
†Corresponding author. E-mail: liuhongping@wipm.ac.cn
© 2010 Chinese Physical Society and IOP Publishing Ltd

emission of the outgoing wave of the valence electron will be confined by three random initial parameters, namely, each launched trajectory will depend on the cosine of the launch angle of the trajectory, the launch time distribution, and the initial energy distribution of the trajectory.[18]

In this paper, using the classical trajectory Monte Carlo (CTMC) method, we investigate how energy and time averaging of the electron wave packets affects the resolution of electron pulses for the ionisation of the Rydberg hydrogen atoms near a metal surface. The energy dependence of the arrival time for each pulse in the ionisation train can help us to design an optimal laser pulse to obtain a certain narrow pulse in the electron train. We illustrate that the excitation to higher N Rydberg states will benefit the generation of narrower electron pulses in the train as well.

2. Theory

Assuming a metal plate located in the $\tilde{z} = -d$ plane and an infinitely massive nucleus charge positioned at the origin of the coordinate system. The Rydberg electron moves in the combined potentials: the Coulomb potential and the electrostatic image potential. The analytical expression of the hydrogen-surface potential can be obtained by electric image method. Considering the cylindrical symmetry, we describe the electron dynamics in a cylindrical coordinate system $(\tilde{\rho}, \tilde{z}, \tilde{\varphi})$. The Hamiltonian for the hydrogen electron has the form (in atomic units):

$$\tilde{H} = \frac{\tilde{p}^2}{2} - \frac{1}{\tilde{r}} + \frac{1}{\sqrt{\tilde{\rho}^2 + (2d + \tilde{z})^2}} - \frac{1}{4(d + \tilde{z})}, \quad (1)$$

where $\tilde{r} = \sqrt{\tilde{\rho}^2 + \tilde{z}^2}$ and $\tilde{p}^2 = \tilde{p}_\rho^2 + l_z^2/\tilde{\rho} + \tilde{p}_z^2$. The last two terms in Eq. (1) are the electrostatic image potential. Owing to the cylindrical symmetry, the $\tilde{z}$-component of angular momentum is conserved and then the $\tilde{\varphi}$-motion can be separated. Thus, we can reduce the electron motion into a two-dimensional problem. Assuming $l_z = 0$, after the scaled transformation, $r = \tilde{r}/d$, $p = \tilde{p}\sqrt{d}$ and $E = \tilde{E}d$, the classical motion of the electron is governed by the scaled Hamiltonian[16]

$$\begin{aligned} H &= \frac{p^2}{2} - \frac{1}{r} + \frac{1}{\sqrt{\rho^2 + (2 + z)^2}} - \frac{1}{4(1 + z)} \\ &\equiv \frac{p^2}{2} + V(\rho, z). \end{aligned} \quad (2)$$

Applying the preceding scalings to the quantum momentum operator, $\tilde{p} = -\mathrm{i}\,\hbar\frac{\partial}{\partial\tilde{q}}$, we can have a scaled version of Planck constant $\hbar_\mathrm{s} = \hbar d^{-1/2} = \hbar(\tilde{E}/E)^{1/2}$. It is expressed in atomic units ($\hbar = 1$) as

$$\hbar_\mathrm{s} = \frac{1}{N\sqrt{2\,|E|}}, \quad (3)$$

where $N = \left(2\left|\tilde{E}\right|\right)^{-1/2}$ is the ersatz principal quantum number. Equation (3) confirms an intuition that when exciting the atom to higher energies, the effective value of Planck constant is lowered and the system will be more 'classical'. The saddle point of the effective potential $V(\rho, z)$ in Eq. (2) is at $\rho_\mathrm{s} = 0$, $z_\mathrm{s} = -0.693673$.[16] If the electron escapes across the saddle point, it will be ionised and recorded by the detector. In this paper, we place the detector at the plane $z = -0.8$.

Using the first-order time-dependent quantum perturbation theory,[19,20] the initial Coulomb eigenstate $|\psi_i>$ generates the excited time-dependent state $|\psi(t)>$ according to:

$$\left[\mathrm{i}\,\hbar_\mathrm{s}\frac{\partial}{\partial t} - H\right]|\psi(t)> = H_L(t)\,\mathrm{e}^{-\mathrm{i}\,E_i t/\hbar_\mathrm{s}}|\psi_i>, \quad (4)$$

in which E_i is the energy of $|\psi_i>$ and $H_L(t)$ describes the interaction between the laser field and the excited electron,

$$H_L(t) = F_L D g(t), \quad (5)$$

where F_L is the peak electric-field strength (in scaled units), D the dipole operator, and $g(t)$ a time dependent function, defined as $g(t) = g_\mathrm{env}(t)\exp(-\mathrm{i}\,\omega_L t)$, with ω_L being the central laser frequency, $g_\mathrm{env}(t) = \exp\left[-t^2/(4\Delta_t^2)\right]$ and Δ_t the standard deviation of the laser pulse intensity. We use the semiclassical approximation theory to describe the outgoing wave.[19]

For the pulsed laser considered here, the outgoing wave $\psi_\mathrm{out}(r)$ is emitted over the time interval Δ_t, determined by $g_\mathrm{env}(t)$. The energy of the wave has a deviation Δ_E at the central energy E_c, which satisfies the uncertainty relation $\Delta_E\Delta_t \geq \hbar_\mathrm{s}/2$. Semiclassically, we model the electron pulse by an ensemble of classical trajectories. The initial distribution of trajectories in the energy–time plane is given by the Wigner function $W_f(E,t)$ of $f(t) = g_\mathrm{env}(t)\exp(-\mathrm{i}\,E_\mathrm{c}t/\hbar_\mathrm{s})$,[15]

$$\begin{aligned} W_f(E,t) &= \int_{-\infty}^{\infty} \mathrm{d}s\mathrm{e}^{\mathrm{i}\,sE/\hbar_\mathrm{s}} f(t + s/2)\, f^*(t - s/2) \\ &= A\mathrm{e}^{-t^2/(2\Delta_t^2)}\mathrm{e}^{-(E-E_\mathrm{c})^2/(2\Delta_E^2)} \end{aligned} \quad (6)$$

with normalization factor $A = 2\sqrt{2\pi}\Delta_t$ and $\Delta_E = \hbar_\mathrm{s}/(2\Delta_t)$. The initial distribution of launch angles θ is given by $|y(\theta)|^2\sin(\theta)$.[20,21]

Within the semiclassical theory, the evolution of the initial wave packet is approximated by following the trajectories within the corresponding classical distribution.[15,20,21] These trajectories are integrated until they reach the detector located at $z = -0.8$, or until the evolution time is beyond the maximum time. The total number of trajectories striking the detector per unit time is then recorded as a function of time. We use atomic units throughout this paper unless stated otherwise.

3. Results and discussion

Figure 1 shows the ionisation rate of the hydrogen atom near the metal surface. The initial angular distribution of electrons is assumed to be s wave for simplicity, with $y = 1$, which weights all directions evenly. The dotted line is calculated at a fixed scaled energy $E = -0.8$ and a precise launch time with $t = 0$, while the thick line is calculated using an ensemble represented by a Gaussian wave packet with $\Delta_t = 0.129$, $\Delta_E = 0.038$ and central energy $E_c = -0.8$. Both lines exhibit a train of pulses and the corresponding orbits are shown above each pulse. All orbits maintain their shapes in the narrow energy range of the laser pulse. For the dotted line, each pulse has a sharp initial arrival time and decays exponentially. The initial arrival time is the earliest time of the corresponding escape segment.[15]

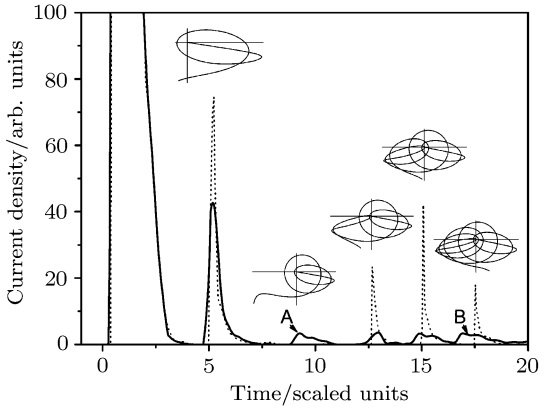


Fig. 1. The ionisation rate of hydrogen atom near the metal surface. The dotted line is calculated at a single fixed scaled energy $E = -0.8$ and a precise launch time $t = 0$. The thick line uses an ensemble represented by Gaussian wave packet with $\Delta_t = 0.129$ and $\Delta_E = 0.038$. The central (physical) energy of the wave packet is $\tilde{E} = 1/(2N^2)$ with $N = 80$. Equivalently, d is 10240 a.u. and the scaled time unit equals to 25 ps. The corresponding trajectories are also shown above. The symbols A, B are explained in the text.

For the thick line, however, the pulses are averaged out although they are still discernible. For the pulse B, the arrival time is not centred on the unaveraged pulse, but it is shifted toward earlier time. This phenomenon will be explained below. Beside the pulse existing in the unaveraged pulse train, a new pulse signatured by A emerges in the average pulse train as well. The corresponding orbit is given birth approximately at $E = -0.78$.

The ionisation rate of the hydrogen atom near the metal surface at scaled energy $E = -0.6$ is given in Fig. 2. Each pulse is averaged out by the uncertainty of the Gaussian wave packet, too. The earliest arrival time of pulse labeled in Fig. 2 is a function of energy, which is shown in Fig. 3. As the energy deceases, the trajectories move faster and tend to strike the detector earlier. For pulses 1 and 2, the behaviour is nearly linear over the energy range plotted. However, pulse 3 shows notable nonlinear behaviour, which is substantially bent. This bending is closely related to the creation of the corresponding trajectory. The pulse is created at $E \approx -0.635$, where it has an infinite arrival time and then it bends into a nearly straight curve. Since the arrival time does vary with energy, we can optimize the resolution of an electron peak in the pulse train by making a balance between the energy spread and the time duration of a laser pulse.[15]

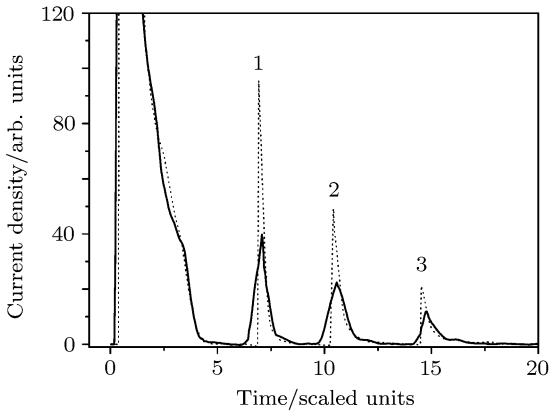


Fig. 2. The ionisation rate of hydrogen atom near the metal surface at scaled energy $E = -0.6$. As in Fig. 1, the dotted line uses an ensemble with precise energy and launch time while the thick line uses a Gaussian wave packet with $\Delta_t = 0.2015$, $\Delta_E = 0.028$. The central (physical) energy of the wave packet is $\tilde{E} = 1/(2N^2)$ with $N = 80$. Equivalently, d is 17680 a.u. and the scaled time unit equals to 16 ps. The numbers 1–3 used to label the peaks are explained in text.

For a given electron pulse, assuming Δ_E is small enough, its curve in Fig. 3 can be approximated by a straight line. In this case, Δ_E will result in a

variation for the arrival time: $\Delta_t^{'} = |b|\,\Delta_E$, where $|b| = (\mathrm{d}t/\mathrm{d}E)_{E=E_c}$ is the inverse slope of the curve in Fig. 3, at the central energy. Thus, the unaveraged pulse is averaged by convolving with two Gaussians of widths Δ_t and $\Delta_t^{'} = |b|\,\hbar_s/(2\Delta_t)$. This is equivalent to convolve with a single Gaussian of width $\Delta_{t,\mathrm{tot}} = \sqrt{\Delta_t^2 + \Delta_t^{'2}}$. While $\Delta_{t,\mathrm{tot}}$ takes a minimum value of $\sqrt{|b|\,\hbar_s}$ at[15]

$$\Delta_t = \Delta_{t,\mathrm{opt}} = \sqrt{\frac{|b|\,\hbar_s}{2}}, \tag{7}$$

$$\Delta_E = \Delta_{E,\mathrm{opt}} = \sqrt{\frac{\hbar_s}{2\,|b|}}. \tag{8}$$

Since the direct pulse is not significantly averaged by the uncertainty of the Gaussian wave packet used, we have computed $\Delta_{t,\mathrm{opt}}$ by evaluating b for the pulse 1. For the scaled energy $E = -0.6$, b will be equal to 13. Since the slope of pulse 2 is similar to that of the pulse 1, all estimations will work well for other pulses.

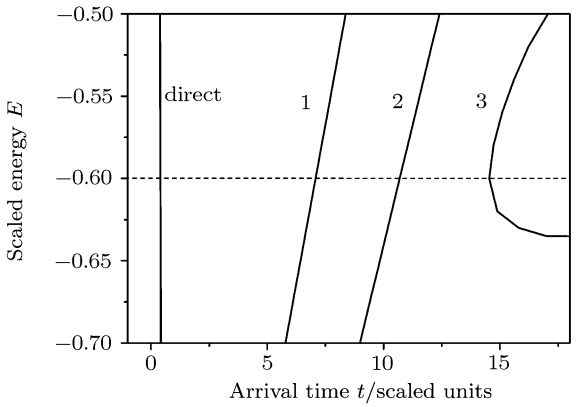


Fig. 3. The earliest arrival time of the pulses labeled in Fig. 2. is shown as a function of energy. For pulses 1 and 2, the curves are closely linear over the energy range plotted. However, pulse 3 displays notable nonlinear behaviour.

In Fig. 4, we compute the ionisation rate for the hydrogen atom near the metal surface at scaled energies $E = -0.6$ with various excitation energy $\tilde{E} = 1/\left(2N^2\right)$. The outgoing electron wave packet is modeled by an ensemble of trajectories with the minimum uncertainty determined by Eqs. (7) and (8) . The physical distance d is simultaneously adjusted to keep the scaled quantities E constant. This leaves the classical Hamiltonian unchanged, but the effective planck constant $\hbar_s$ decreases by $1/N$. Thus, the extension of the Gaussian wave packet in the energy–time plane decreases by $1/N$ and the energy–time-averaged pulse train will be closer to the unaveraged pulse train.[15] Figure 4 shows the pulse trains for $N = 20, 80, 400$. In each case, the width of the averaged electron pulse is dependent on $\Delta_{t,\mathrm{tot}}$, which scales as $1/\sqrt{N}$. As shown in Fig. 4, rather than centring on the unaveraged pulse 3, the energy–time-averaged pulse 3 shifts toward larger time. This can be understood by examining the arrival time curve in Fig. 3. At the central energy $E_c = -0.6$, a Gaussian distribution of energies at E_c has equal weights above the dashed line as below. However, the variation in arrival time above the line is smaller than the variation below the line, since the curve is bent to infinity below E_c. Therefore, the energy-averaged pulse tends to pile up at a time falling behind the unaveraged pulse.

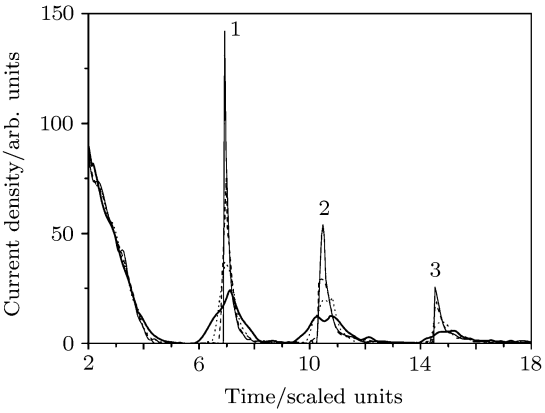


Fig. 4. The ionisation rate for hydrogen atom near the metal surface at scaled energy $E = -0.6$ for different excitation energy $\tilde{E} = 1/\left(2N^2\right)$. The thin line is the unaveraged pulse train, while the thick line is the averaged one for $N = 20$, $\Delta_t = 0.5444$, $\Delta_E = 0.0419$, $d = 480$ a.u. and t scale= 0.254 ps; dashed curve for $N = 80$, $\Delta_t = 0.2722$, $\Delta_E = 0.0209$, $d = 7680$ a.u. and t scale= 16.28 ps; and dotted curve for $N = 400$, $\Delta_t = 0.1233$, $\Delta_E = 0.0094$, $d = 192000$ a.u. and t scale= 2.035 ns.

4. Conclusion

We have investigated the ionisation rate of the hydrogen atom near the metal surface, excited by a pulse laser. The outgoing wave packet is initialized as an ensemble of electron with an initial launch time distribution and an initial energy distribution. In real experiment, the applied laser pulse has a non-zero pulse duration and the ionisation pulse will not be simply a sharp peak with an exponentially decaying tail. As the arrival time of each electron pulse is energy-dependent, the actual ionisation pulse train will be averaged by the uncertainty of the wave packet. However, a detailed calculation can help us to optimize the Gaussian wave packet to arrive at a certain narrow peak in the ionisation pulse train. We also investigate the effect of different excitation energy on the ionisation electron pulse train and find that the excitation to higher N Rydberg states will produce narrower electron pulse train in the ionisation as well.

References

[1] Landau L D and Lifshitz E M 1979 *Quantum Mechanics: Nonrelativistic Theory* (New York: Pergamon)

[2] Alber G, Ritsch H and Zoller P 1986. *Phys. Rev.* A **34** 1058.

[3] Broers B, Christian J F and van Linden van den Heuvell H B 1994 *Phys. Rev.* A **49** 2498

[4] Mitchell K A, Handley J P, Tighe B, Flower A and Delos J B 2004 *Phys. Rev. Lett.* **92** 073001

[5] Nicole C, Sluimer I, Rosca-Pruna F, Warntjes M, Vrakking M, Bordas C, Texier F and Robicheaux F 2000 *Phys. Rev. Lett.* **85** 4024

[6] ten Wolde A, Noordam L D, Lagendijk A and van Linden van den Heuvell H B 1988 *Phys. Rev. Lett.* **61** 2099

[7] Yeazell J A and Stroud Jr C R 1988 *Phys. Rev. Lett.* **60** 1494

[8] Yeazell J A, Mallalieu M and Stroud C R 1990 *Phys. Rev. Lett.* **64** 2007

[9] Lankhuijzen G M and Noordam L D 1996 *Phys. Rev. Lett.* **76** 1784

[10] Yeazell J A and Stroud C R 1987 *Phys. Rev.* A **35** 2806

[11] Molander W A, Stroud C R and Yeazell J A 1986. *J. Phys.* B **19** L461

[12] Nicole C, Offerhaus H L, Vrakking M J J, Lépine F and Bordas C 2002 *Phys. Rev. Lett.* **88** 133001

[13] Blondel C, Delsart C and Dulieu F 1996 *Phys. Rev. Lett.* **77** 3755

[14] Deng S H, Gao S, Li Y P, Xu X Y and Lin S L 2010 *Chin. Phys.* B **19** 040511

[15] Mitchell K A, Handley J P, Tighe B, Flower A and Delos J B 2004 *Phys. Rev.* A **70** 043407

[16] Wang D H, Huang K Y and Lin S L 2009 *Euro. Phys. J.* D **54** 699

[17] Bordas C, Lépine F, Nicole C and Varkking M J J 2003 *Phys. Rev.* A **68** 012709

[18] Topçu T and Robicheaux F 2007 *J. Phys.* B **40** 1925

[19] Haggerty M R and Delos J B 2000 *Phys. Rev.* A **61** 053406

[20] Du M L and Delos J B 1987 *Phys. Rev. Lett.* **58** 1731

[21] Du M L and Delos J B 1988 *Phys. Rev.* A **38** 1913